

Supplementary information

Novel carbon and sulfur tolerant anode material FeNi_3 @ $\text{PrBa}(\text{Fe,Ni})_{1.9}\text{Mo}_{0.1}\text{O}_{5+\delta}$ for IT-SOFCs

Shuangshuang Xue,^a Nai Shi,^a Yanhong Wan,^a Zheqiang Xu,^a Daoming Huan,^a Shaowei Zhang,^a Changrong Xia,^a Ranran Peng,^{*a,b,c} Yalin Lu^{*a,b,c,d}

^a Science and Engineering, University of Science and Technology of China, Hefei, 230026 Anhui, China.

^b Synergetic Innovation Center of Quantum Information & Quantum Physics, University of Science and Technology of China, Hefei, Anhui 230026, China.

^c Hefei National Laboratory of Physical Science at the Microscale, University of Science and Technology of China, Hefei, 230026 Anhui, China.

^d National Synchrotron Radiation Laboratory, University of Science and Technology of China, Hefei 230026, P. R. China.

*. Corresponding author.

Table. S1 Rietveld refinement results for PBFMNi0.3 and FeNi₃@PBFMNi0.3 samples: lattice parameters and

Sample	Space group	a (Å)	b (Å)	c (Å)	R _{wp} (%)	R _p (%)	χ ²
PBFMNi0.3	Pm-3m	3.905	3.905	3.905	7.27	5.10	2.71
FeNi ₃ @PBFMNi0.3	Pm-3m	3.938	3.938	3.938	6.89	5.15	3.20

corresponding fitting errors

Table. S2 Oxygen partial pressure (P_{O2}) of humidified 5% H₂/Ar and 10% H₂/Ar at different temperatures.

Temperature (°C)	P _{O2} (atm)	
	5% H ₂ /Ar	10% H ₂ /Ar
550	7.93×10^{-27}	1.98×10^{-27}
600	4.93×10^{-25}	1.23×10^{-25}
650	1.97×10^{-23}	4.91×10^{-24}
700	5.41×10^{-22}	1.35×10^{-22}
750	1.07×10^{-20}	2.69×10^{-20}

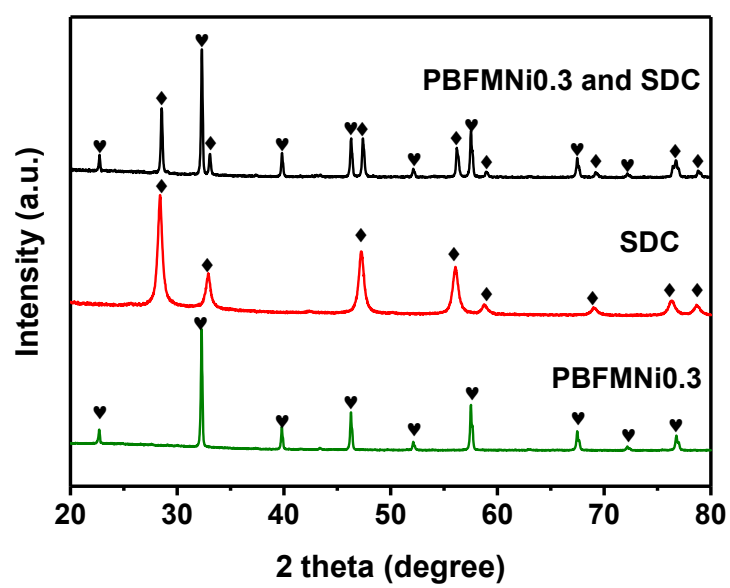


Figure. S1 RT-XRD patterns for PBFMNi0.3 powders, SDC powders and their mixtures calcined at 1000 °C in air for 2 hours.



Figure. S2 TEM image of FeNi₃@PBFMNi0.3

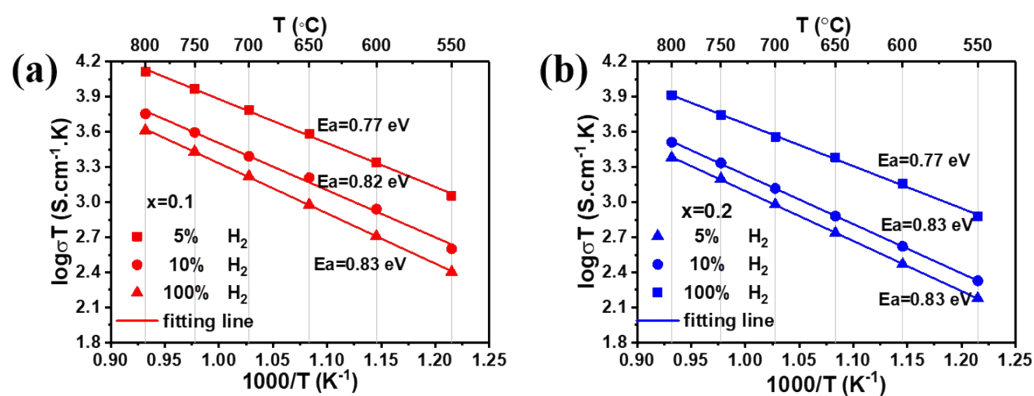


Figure. S3 Arrhenius plots of conductivities for (a) FeNi₃@PBFMNi_{0.1} and (b) FeNi₃@PBFMNi_{0.2} measured at 550-800 °C in wet 5% H₂/Ar, 10% H₂/Ar and 100% H₂, respectively.

ECR technique is based on the equilibrium relationship between the electrical conductivity and the oxygen concentration of nonstoichiometric oxide materials. The conductivity evolution of a sample after an abrupt change in P_{O_2} of the ambient atmosphere is recorded as a function of time. A typical model used to estimate surface oxygen

exchange coefficient (k_{chem}) and oxygen diffusion coefficient (D_{cnem}) in ECR analysis is to solve the linear diffusion equation (Fick's second law) with linear absorbing boundary conditions. The corresponding analytical solution is given by

$$g(t) = \frac{\sigma(t) - \sigma(0)}{\sigma(\infty) - \sigma(0)} = \frac{c(t) - c(0)}{c(\infty) - c(0)} = 1 - \sum_{m=1}^{\infty} \sum_{n=1}^{\infty} \sum_{p=1}^n \frac{2L_{\beta}^2 \exp\left(-\beta_m^2 Dt/x^2\right)}{\beta_m^2 (\beta_m^2 + L_{\beta}^2 + L_{\gamma})} \times \frac{2L_{\gamma}^2 \exp\left(-\gamma_n^2 Dt/y^2\right)}{\gamma_n^2 (\gamma_n^2 + L_{\gamma}^2 + L_{\phi})}$$

Where $g(t)$ is the normalized conductivity, $\sigma(0)$ and $\sigma(\infty)$ represent the initial and final conductivities, respectively, and $c(0)$ and $c(\infty)$ are the corresponding oxygen concentrations. Parameters x , y and z are the sample dimensions, while $\beta_m, \gamma_n, \phi_p$ are the positive, non-zero roots of

$$\beta_m \tan \beta_m = L_{\beta}; \gamma_n \tan \gamma_n = L_{\gamma}; \phi_p \tan \phi_p = L_{\phi}$$

The eigenvalues

$$L_{\beta} = \frac{x}{L_c}; L_{\gamma} = \frac{y}{L_c}; L_{\phi} = \frac{z}{L_c}$$

Where

$$L_c = \frac{D_{cnem}}{k_{chem}}$$

The parameters obtained from fitting are the chemical surface exchange coefficient, k_{chem} (m.s^{-1}) and the chemical diffusion coefficient, D_{cnem} ($\text{m}^2.\text{s}^{-1}$). When the sample is thin enough, which often means its thickness is smaller than the characteristic thickness L_c , the diffusion step is so fast that the incorporation reaction is limited only by the surface exchange. What's more, the relative change of the oxygen concentration as a function of time is

$$\frac{\partial c(t)}{\partial t} = - \frac{S k_{chem}}{t} [c(t) - c(0)]$$

In this case, the normalized conductivity obtained in experiment is fitted with the surface exchange controlling E

$$g(t) = \exp\left(-\frac{S}{V} k_{chem} t\right)$$

exponential function

Where S (m^2) is the sample surface area and V (m^3) is the sample volume.

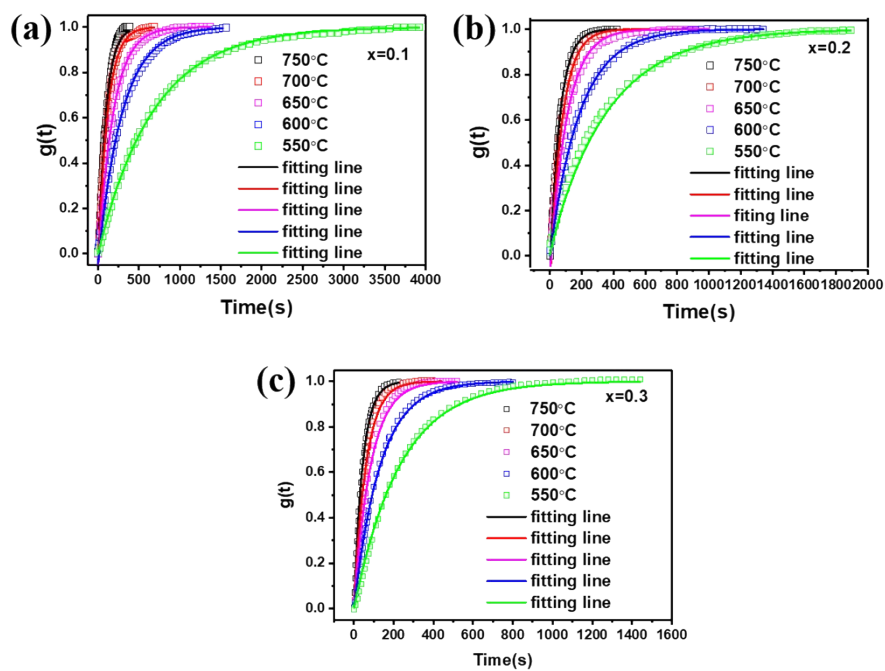


Figure. S4 Electrical conductivity relaxation curves of (a) FeNi₃@PBFMNI0.1, (b) FeNi₃@PBFMNI0.2 and (c) FeNi₃@PBFMNI0.3 at 550-750 °C

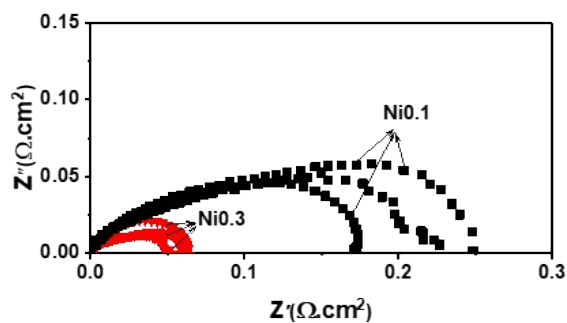


Figure. S5 EIS of button cells using PBFMNI0.1-SDC (black) and PBFMNI0.3-SDC (red) anodes, respectively, operating in wet H₂.

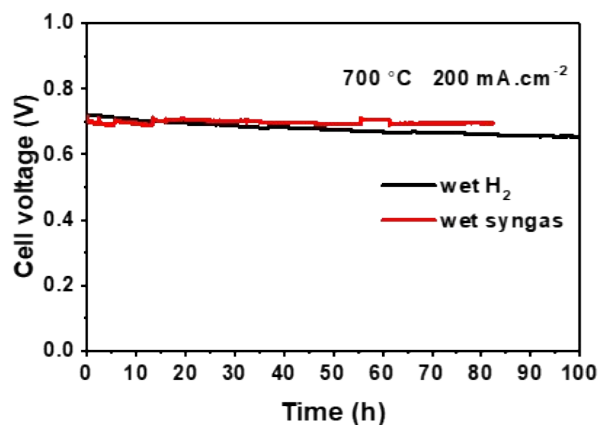


Figure. S6 Cell voltage as a function of testing time for single-cell PBFMNi0.3-SDC|SDC|LSCF-SDC operated under a constant current density of 200 mA cm^{-2} at 700°C .

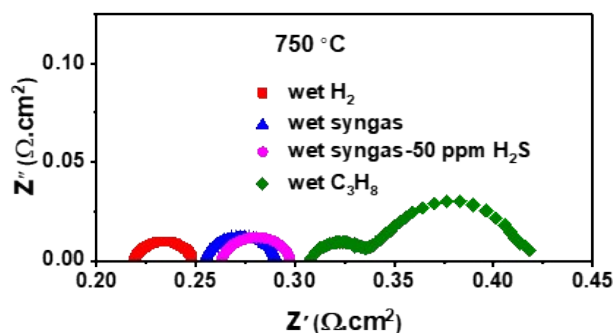


Figure. S7 EIS of SDC electrolyte-supported single-cell PBFMNi0.3-SDC|SDC|LSCF-SDC operating in wet H_2 , wet propane, wet syngas and syngas-50 ppm H_2S , respectively at 750°C .

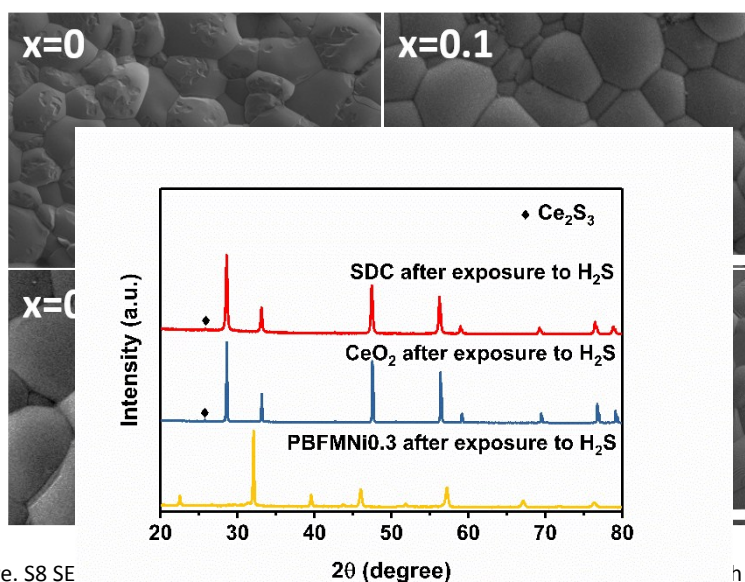


Figure. S8 SE

h in air.

Figure S9 XRD patterns for PBFMNi0.3 powders, CeO_2 powders and SDC powders after exposure to H_2 with 50 ppm H_2S for 20 h at 750°C



Figure. S10 the SEM images: (a) Cross-sectional view of a whole cell consisting of a PBFMNi0.3-SDC anode and a LSCF-SDC cathode; (b) a PBFMNi0.3-SDC anode and a SDC dense electrolyte; (c) a PBFMNi0.3-SDC anode; (d) Cross-sectional view of a whole cell after 100 h long-term test in syngas with 50 ppm H₂S; (e) a FeNi₃@PBFMNi0.3-SDC anode and a SDC dense electrolyte after 100 h long-term test in syngas with 50 ppm H₂S; (f) FeNi₃@PBFMNi0.3-SDC anode after long term test in syngas with 50 ppm H₂S.